



Performance Analysis of Parabolic Trough Collector in Hot Climate

Adel A. Ghoneim^{1*}, Adel M. Mohammedein¹ and Kandil M. Kandil¹

¹Applied Sciences Department, College of Technological Studies, Public Authority for Applied Education and Training (PAAET), P.O. Box 42325, Shuwaikh 70654, Kuwait.

Authors' contributions

This work was carried out in collaboration between all authors. Authors AAG, AMM and KMK designed the study, performed the statistical analysis, wrote the protocol and wrote the first draft of the manuscript and managed literature searches. All authors read and approved the final manuscript.

Original Research Article

Received 30th December 2013

Accepted 12th March 2014

Published 22nd March 2014

ABSTRACT

In most existing buildings cooling and heating loads lead to high primary energy consumption and, consequently, high CO₂ emissions. These can be substantially decreased with suitable energy concepts using appropriate integrated renewable systems. In the present study a numerical model is developed to study the effect of different collector parameters and operating conditions on the performance of parabolic trough solar collector (PTSC) in Kuwait climate. The proposed model takes into consideration the thermal interaction between absorber-envelope, and envelope-envelope for thermal radiation losses which have been neglected in existing models. A review of the equations for convective heat transfer losses was performed as well and new equations were developed and used in the present model. The effects of heat conduction in the collector tube wall and mixed convection in the inner tube, which have been neglected in previous studies, are included in the proposed model. In addition, a case study is carried out adapting parabolic trough collectors to satisfy nominal space heating load, water heating load and cooling load of a typical Kuwaiti dwelling. Finally, the environmental impact of solar heating and cooling systems under Kuwait climate conditions is investigated. Present results indicate that convection loss from the absorber tube to supporting structures is the largest among the other losses (conduction and radiation). Also, at noon time PTSC has the smallest angle of incidence and the highest efficiency and when the annulus between the receiver surface and the glass envelope is

*Corresponding author: E-mail: aa.ghoniem@paaet.edu.kw;

In vacuo, conduction and convection across the annulus are effectively eliminated. In addition, space heating load and domestic water heating load can be completely provided by PTSC. The minimum required collector area is about 82 m² to supply cooling loads of a typical residential house under all climatic conditions in Kuwait. A CO₂ emission reduction of about 12.3tonne/year can be achieved as a result of adapting parabolic trough solar collector to a typical Kuwaiti dwelling.

Keywords: Parabolic trough collector; building integrated renewable systems; solar fraction.

1. INTRODUCTION

Energy consumption worldwide is increasing rapidly due to increasing global population and industrialization processes in many countries. The production and use of conventional fossil fuel energy resources account for a high percentage of the air pollution, leading to harmful impact on our environment. In contrast, renewable energy sources can be adapted to produce energy sources with little -if any- pollution. Widespread commercialization of renewable energy systems, specially in hot weather regions like Kuwait, can significantly reduce consumption of conventional fuels. In return, this will help greatly in reducing pollution and maintain our environment healthy and clean. Concentrating solar power (CSP) technologies now constitute feasible commercial options for large scale power plants as well as for smaller electricity and heat generating devices.

There are currently four basic commercially available CSP technologies. These plants typically consist of three main circuits: The Solar Field, through which the heat transfer fluid (HTF) circulates, the Power Block, which circulates water and steam, and the Thermal Storage System (TES) system. The HTF and water-steam circuits and the HTF and TES circuits can exchange energy at the corresponding heat exchangers.

Parabolic trough collector is a type of high temperature solar concentrator collector. These collectors have a linear parabolic shaped reflector that focuses sun radiation on a receiver at the focus of the reflector. Parabolic troughs are long parallel rows of curved glass mirrors. Mirrors are usually silver coated or polished aluminum, focusing the sun's energy on an absorber pipe located along its focal line. Parabolic trough collectors use high temperatures to heat up a fluid in absorber tubes arranged in the focal line. The heat transfer fluid (HTF), usually oil, is circulated through the pipes. Under normal operation, the heated HTF leaves the collector with a specified collector outlet temperature and is pumped to a central power plant area. There, the HTF is passed through several heat exchangers where its energy is transferred to the power plant's working fluid, which is usually steam. The heated steam is used in turn to drive a turbine generator to produce electricity. Thermal storage can be used to provide electricity during peak hours or when sun intensity is low. Solar collector tube is a key component in parabolic trough solar thermal generation system. It is used to convert solar radiation to thermal energy. Optimizing its performance and improving its efficiency has important effects on the thermal-electricity conversion efficiency.

Kalogirou et al. [1] studied the performance of parabolic trough collectors using a theoretical model. They predicted the quantity of steam generated by the system. The optimum flash vessel diameter and inventory obtained from this analysis are 65 mm and 0.71, respectively. Current state of the art of parabolic trough solar power technology is reviewed by Price et al. [2]. They described the research efforts that are in progress to enhance this technology. They claimed that since the last commercial parabolic trough plant was built, substantial

technological progress has been attained. The review shows how the economics of future parabolic trough solar power plants is expected to improve. Riffelmann et al. [3] developed two methods to measure the solar flux in the focal region of parabolic trough collector. Intercept losses are detected and assigned to the locations on the parabola from which they are caused. Direct steam generation in parabolic trough collectors were studied and reported by Eck et al. [4]. They presented the advantages, disadvantages, and design considerations of a steam cycle operated with saturated steam. A simulation study of solar lithium bromide–water absorption cooling system with a parabolic trough collector is carried out by Mazloumi et al. [5]. The system has been designed to supply the cooling load of a typical house with a cooling load peak is of about 17.5 kW (5 tons of refrigeration), which occurs in July. The minimum required collector area was estimated at 57.6 m², enough to supply the cooling loads for peak energy consumption.

A reflux heat transfer storage concept for producing high-temperature superheated steam in the temperature range 350–400°C was developed and tested by Adinberg et al. [6]. The thermal storage medium is a metallic substance, Zinc–Tin alloy, which serves as the phase change material. A high-temperature heat transfer fluid is added to the storage medium in order to enhance heat exchange within the storage system. At the same time, the associated heat exchangers serve for charging and discharging the storage. The tests produced satisfactory results in terms of thermal stability and compatibility of the utilized storage materials up to a working temperature of 400°C. Garcia et al. [7] presented an overview of the parabolic-trough collectors built and marketed during the past century, as well as the prototypes currently under development. In addition, they presented a survey of systems which could incorporate this type of concentrating solar system to supply thermal energy up to 400°C, specially steam power cycles for electricity generation.

Sansoni et al. [8] investigated parabolic trough collectors and applied the study results to a plant prototype installed in Florence (Italy) for residential supply. Their work summarizes the results of several studies. It also analyzes the interactions between collection efficiency, angular misalignments, mirror deformations, sun tracking and trough placement. They concluded that the placement of a parabolic trough collector and sun tracking should be matched to optimize the collection performance. Daniel et al [9] employed selective coatings with evacuated and non evacuated glass tubes to control radiative and convective heat losses. They developed a numerical technique to investigate the performance of the vacuum shell. Their study revealed that the performance of the evacuated tube with selective coating is the highest amongst all configurations.

A detailed heat transfer analysis and modeling of a parabolic trough solar receiver were carried out by Forristall [10]. One and two dimensional energy balances were used for short and long receivers, respectively. A model was used to determine the thermal performance of parabolic trough collectors under different operating conditions. Jones et al. [11] carried out a comprehensive model of 30 MWe SEGS VI parabolic trough plant. The model was created to accurately predict the SEGS VI plant behavior and to examine transient effects such as startup, shutdown and system response. Li Xu et al. [12] developed a comprehensive physical model to predict the thermal performance of parabolic trough collectors during transient operations. Four sets of outdoor tests were conducted to verify the model using a 100 m long row of parabolic trough solar collectors. Comparison of the predicted outlet temperature, energy output and thermal efficiency with measured data shows that the model accurately predicts the transient thermal performance for both heating and cooling processes.

A thermal economic model called Solar Advisor Model (SAM) was developed by NREL and Sandia National Laboratory [13,14]. This model calculates costs, finances, and performance of concentrating solar power and also allows examining the impact of variation in physical parameters on costs and overall performance. A more recent methodology for the economic optimization of the solar area in either parabolic trough or complex solar plants was carried out by Montes et al. [15]. An analytic model of a solar thermal electric generating system with parabolic trough collectors was carried out by Rolim et al. [16]. A simplified numerical methodology for designing parabolic trough solar energy systems was proposed by Stine and Harrigan [17]. This method proposed a design chart called storage sizing graph, which obtains the optimum collector area for certain locations.

Edenburn [18] predicted the efficiency of a PTC by using an analytical heat transfer model for evacuated and non evacuated annulus cases. The results showed good agreement with measured data obtained from Sandia National Laboratories collector test facility [19]. Ratzel et al. [20] carried out both analytical and numerical studies of the heat conduction and convective losses in an annular receiver for different geometries. Three techniques were proposed to reduce the conduction heat loss: evacuation, over sizing annular receiver while keeping the Rayleigh number below 1000 over operation range and use of gases with low thermal conductivity. Dudley et al. [21] developed an analytical model of SEGS LS-2 parabolic solar collector. The thermal loss model for the heat collection element was one dimensional steady state model based on thermal resistance analysis.

Stuetzle [22] proposed an unsteady state analysis of the solar collector receiver to calculate the collector field outlet temperature. The results show a good match between the calculated and measured outlet temperatures. García-Valladares and Velásquez [23] developed a detailed numerical model for single pass solar receiver and validated it. Their results showed that the proposed configuration enhances the thermal efficiency of the solar collector compared with single pass. Heidemann et al. [24] formulated a two dimensional heat transfer model for calculating the absorber wall temperature of a parabolic trough collector under steady and unsteady conditions. The numerical solution showed that a sudden drop of irradiation induces a very high temperature gradient inside the absorber tube in a short period of time. Odeh et al. [25] carried out a model research for heat loss of a parabolic trough collector in terms of wall temperature rather than working fluid temperature. Their results were compared with the Sandia test data and showed that the model underestimates the measured loss. Recently, three dimensional heat transfer analysis of PTCs was performed by combining the Monte Carlo Ray Trace Method (MCRT) and CFD analysis [26-28]. The results indicated that the support bracket and bellow under non-vacuum conditions bring a high conductive heat loss.

The foregoing literature review shows that a lot of studies have been carried out to model the performance of parabolic trough collectors. However, existing models assume that there is no thermal interaction between the neighboring surfaces (absorber-envelope, and envelope-envelope) for thermal radiation losses. The previous assumptions greatly simplify the analysis. However, these assumptions underestimate the radiation losses at high absorber temperatures. To account for the thermal interaction between adjacent surfaces, a comprehensive radiative analysis is implemented in the present study for heat losses in the absorber and the glass envelope. A review of the equations for convective heat transfer losses was performed as well and new equations are implemented in the present model. The effects of heat conduction in the collector tube wall and mixed convection in the inner tube which have been neglected in previous studies are also taken into consideration in the proposed developed model. The proposed model can predict the effects of annuli space,

tube diameter ratio and heat conductivity coefficient of the inner tube wall on the heat transfer performance. Parametric studies are carried out for different: collector absorber areas, overall heat loss coefficients, optical losses, collector inlet temperatures, mass flow rates of the heat transfer fluid, angles of incidence and concentration ratios. This will certainly lead to the optimum parabolic trough performance as well as the maximum annual energy yield under Kuwait climatic conditions.

In addition, a case study was carried out adapting parabolic trough collectors to satisfy nominal space heating, water heating and cooling loads for a typical Kuwaiti dwelling as a model for existing buildings. The aim can be set towards achieving nearly zero energy budget buildings in Kuwait. Finally, the environmental impact of solar heating and cooling systems under Kuwait climatic conditions is investigated.

2. THEORETICAL ANALYSIS

2.1 Solar Radiation

Prediction of collector performance requires knowledge of the absorbed solar energy by the collector absorber plate. The solar energy incident on a tilted collector consists of three different components: Beam radiation, diffuse radiation, and ground-reflected radiation. The details of the calculation depend on which diffuse-sky model is used. Using an isotropic sky model, the absorbed radiation on the absorber plate can be expressed as:

$$G = G_b R_b (\tau\alpha)_b + G_d (\tau\alpha)_d \frac{1 + \cos\beta}{2} + (G_b + G_d) (\tau\alpha)_g \rho_g \frac{1 + \cos\beta}{2} \quad (1)$$

Where the subscripts b, d, and g represent beam, diffuse, and ground-reflected radiation, respectively. G is the intensity of radiation on a horizontal surface, $(\tau\alpha)$ the transmittance-absorptance product that represents the effective absorptance of the cover-plate system, β the collector slope, ρ_g is the diffuse reflectance of ground and the geometric factor R_b is the ratio of beam radiation incident on a tilted surface to that on a horizontal surface. The angle of incidence (θ) represents the angle between the beam radiation and plane normal to the surface. There are other losses from the collector due to the angle of incidence. The losses occur because of additional reflection and absorption by the glass envelope as the angle of incidence increases. The angle of incidence modifier (IAM) corrects for these additional reflection and absorption losses.

The calculation can be simplified by defining equivalent angles that give the same transmittance for diffuse and ground-reflected radiation. Performing the integration of the transmittance over the appropriate angle of incidence with an isotropic sky model and equivalent angle of incidence for diffuse radiation yields:

$$\theta_{d,e} = 59.7 - 0.1388 \beta + 0.001497 \beta^2 \quad (2)$$

where β is the tilt angle of the solar collector. For ground-reflected radiation, the equivalent angle of incidence is given by:

$$\theta_{g,e} = 90 - 0.5788 \beta + 0.002693 \beta^2 \quad (3)$$

2.2 Parabolic Trough Collector

A performance model is developed for solar thermal collector based on a linear, tracking parabolic trough reflector. The reflector is focused on a surface-treated metallic pipe receiver enclosed in an evacuated transparent tube. The developed PTSC model is a steady-state model and is based on the energy balance and heat transfer mechanism within PTSC's receiver tube. The model can calculate the fraction of the incident solar energy recovered in the fluid circulating through the pipe receiver, and evaluate the thermal loss from the collector. The model also calculates the pressure drop over the receiver, and the temperature of the various collector components and of fluid throughout the receiver under different conditions. So, the model can be used for optimizing PTSC design by varying the size of the receiver tube, the size of the glass envelope, receiver tube material, coating material and so forth. In addition, the proposed model considers the effect of fluid properties, ambient and operating conditions on the performance of the collector.

The heat collection element (HCE) consists of an absorber surrounded by a glass envelope. The absorber is typically a stainless steel tube with a selective absorber surface which provides the required optical and radiative properties. Selective surfaces combine a high absorptance of solar radiation with low emittance for the temperature range in which the surface emits radiation. The glass envelope is an anti reflective evacuated glass tube which protects the absorber from degradation and reduces heat loss. The vacuum enclosure is used primarily to reduce heat loss at high operating temperatures and to protect the solar-selective absorber surface from oxidation. The heat transfer model is based on an energy balance between the heat transfer fluid and the environment.

The solar energy reflected by the mirror is absorbed mainly by the glass envelope \dot{Q}_{e-abs} and the absorber surface \dot{Q}_{a-abs} . Part of the energy taken by the absorber is transferred to the heat transfer fluid by forced convection $\dot{Q}_{a-f,conv}$, the remaining energy is transferred back to the glass envelope by radiation $\dot{Q}_{a-e,rad}$ and natural convection $\dot{Q}_{a-e,conv}$ and lost through the support brackets by conduction $\dot{Q}_{cond;bracket}$ as well. The heat loss from the absorber in the form of radiation and natural convection is conducted by the glass envelope and lost to the environment by convection $\dot{Q}_{e-sa,conv}$ and radiation $\dot{Q}_{e-s,rad}$, together with the energy absorbed by the glass envelope \dot{Q}_{e-abs} . In order to obtain the partial differential equations that govern the heat transfer phenomena, an energy balance is applied over a section of the solar receiver. The detailed analysis of the partial differential equations and method of solution can be found in Rohsenow et al. [29]. After applying the energy balance on a control volume, assuming unsteady state and incompressible fluid, the following partial differential equation can be obtained:

$$A_{i,a}\rho_f C_{p,f} \frac{\delta T_f}{\delta t} = \dot{m}_f \frac{\delta}{\delta z} C_{p,f} T_f + \frac{V_f^2}{2} + \dot{Q}_{a-f,conv} \quad (4)$$

$$V_f = \frac{\dot{m}_f}{\rho_f A_{i,a}} \quad (5)$$

where \dot{m}_f is the fluid mass flow rate, $A_{i,a}$ is the internal cross sectional area of the absorber, T_f is the fluid temperature, and $\dot{Q}_{a-f,conv}$ is the heat transfer by convection from the absorber to HTF per unit length and is given by:

$$\dot{Q}_{af,conv} = \pi Nu_f k_f (T_a - T_f) \quad (6)$$

where Nu_f is the Nusselt number, k_f is the thermal conductivity of HTF, and T_a is the absorber wall temperature. The equation for fully developed turbulent flow ($Re_D > 2300$) and convective heat transfer in circular ducts introduced by Kakaç et al. [30] is adapted:

$$Nu_f = \frac{(C_f/2)(Re_D/1000)Pr}{1+12.7(C_f/2)^{1/2}(Pr^{2/3}-1)} \left(\frac{Pr}{Pr_w}\right)^{0.11} \quad (7)$$

$$Re_D = \frac{V_f D_{i,a}}{\nu_f} \quad (8)$$

where C_f is the friction coefficient (Fanning friction factor), Re_D is the Reynolds number based on the absorber inner pipe diameter ($D_{i,a}$), Pr is the Prandtl number, and ν_f is the kinematic viscosity of HTF. This equation is valid for $2300 \leq Re_D \leq 5 \times 10^6$ and $0.5 \leq Pr \leq 2000$. The thermal properties should be evaluated at the bulk mean heat transfer fluid temperature, except Pr_w which is evaluated at the absorber wall temperature. The convection heat transfer coefficient for rough tubes can be estimated using the friction coefficient from Colebrook and White as referred by Rohsenow et al. [29]:

$$\frac{1}{\sqrt{C_f}} = 3.48 - 1.7372 \ln \left(\frac{2\varepsilon}{D_{i,a}} + \frac{9.35}{Re_D \sqrt{C_f}} \right) \quad 5 \leq Re_\varepsilon \leq 70 \quad (9)$$

$$\text{With } Re_\varepsilon = \frac{V_f \varepsilon}{\nu_f} \quad (10)$$

For laminar flow, ($Re_D \leq 2300$), the Nusselt number on walls with uniform temperature is given by $Nu_f = 3.66$. Two heat transfer mechanisms occur between the absorber and the glass envelope: convection heat transfer and thermal radiation. Convection heat transfer depends on the annulus pressure; experimental work as stated in Rohsenow et al. [29] has shown that heat transfer loss is independent on the annulus vacuum pressure for pressures above 1Torr. At pressures below 1Torr, molecular conduction is the heat transfer mechanism while for pressure above 1Torr, natural convection takes place. Fig. 1 shows the control volume used for the absorber analysis.

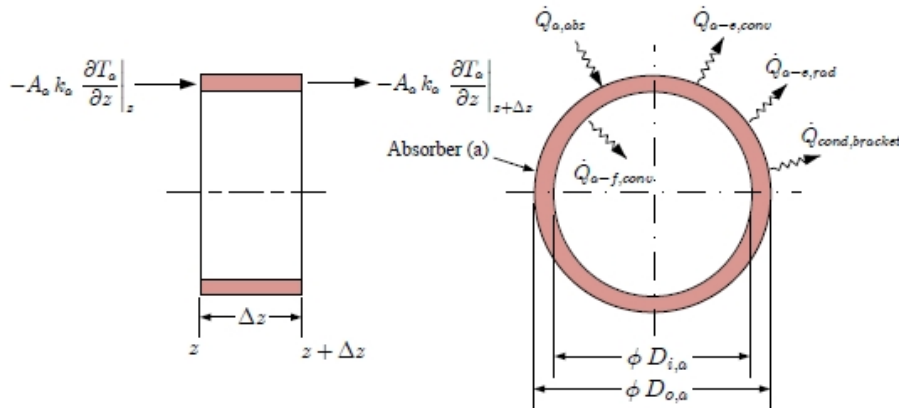


Fig. 1. Control volume for absorber analysis

Applying the energy balance on the control volume:

$$A_a \rho_a C_{p,a} \frac{\delta T_a}{\delta t} = A_a \frac{\delta}{\delta z} k_a \frac{\delta T_a}{\delta z} + \dot{Q}'_{a,abs} - \dot{Q}'_{a-f,conv} - \dot{Q}'_{a-e,conv} - \dot{Q}'_{a-e,rad} - \dot{Q}'_{cond,bracket} \quad (11)$$

where A_a is the absorber cross section area, $A_a = (\pi/4)(D_{o,a}^2 - D_{i,a}^2)$, $D_{o,a}$ is the outer pipe diameter, $D_{i,a}$ is the inner pipe diameter, $\dot{Q}'_{a,abs}$ is the solar absorption in the absorber per receiver length, $\dot{Q}'_{a-f,conv}$ is the heat transfer by convection from absorber to heat transfer fluid per unit length, $\dot{Q}'_{a-e,conv}$ is the heat transfer by convection from absorber to envelope per unit length, $\dot{Q}'_{a-e,rad}$ is the heat transfer by radiation from absorber to glass envelope per unit length, and $\dot{Q}'_{cond,bracket}$ is the heat conduction through support brackets per unit length. Stainless steel is normally used as the absorber tube material. Thermal radiation analysis for one surface implies that all surfaces that can exchange radiative energy with the surface must be considered simultaneously. How much energy two surfaces exchange depends on their size, separation distance and orientation. In order to carry out the radiative heat transfer analysis, the view factors for a short annulus proposed by Siegel and Howell [31] are employed. The heat transfer mechanisms from the glass envelope to the surroundings are convection and radiation. Convection heat transfer distinguish two cases: Wind guided (forced convection) and no wind (natural convection). The radiation heat transfer is basically between the glass envelope and either the sky or the collector surface. The maximum radiation heat loss takes place when the solar receiver is assumed to be surrounded only by the sky. The energy balance on the control volume results in the following partial differential equation:

$$A_e \rho_e C_{p,e} \frac{\delta T_e}{\delta t} = A_e \frac{\delta}{\delta z} k_e \frac{\delta T_e}{\delta z} + \dot{Q}'_{e,abs} + \dot{Q}'_{a-e,conv} + \dot{Q}'_{a-e,rad} - \dot{Q}'_{e-sa,conv} - \dot{Q}'_{e-s,rad} \quad (12)$$

where $\dot{Q}'_{e,abs}$ is the solar absorption in the envelope per receiver length, $\dot{Q}'_{a-e,conv}$ is the heat transfer by convection from the glass envelope to the surrounding air per unit length, and, $\dot{Q}'_{e-s,rad}$ is the heat transfer by radiation from the glass envelope to the sky per unit length. The heat transfer by convection per unit length from the glass envelope to the surrounding air is calculated as:

$$\dot{Q}'_{e-sa,conv} = h_e \pi D_{o,e} (T_e - T_\infty) \quad (13)$$

$$\text{with } h_e = \frac{Nu_e k_e}{D_{o,e}} \quad (14)$$

For no wind conditions, Kakaç et al. [30] recommended the following expression for a horizontal cylinder under natural convection:

$$Nu_e = \left[0.60 + 0.387 \left\{ \frac{Ra_D}{\left[1 + (0.559/Pr)^{9/16} \right]^{16/9}} \right\}^{1/6} \right]^2 \quad (15)$$

In order to simplify the model, it is assumed that half of the receiver surface is surrounded by the mirror and the other half by the sky. The heat flux and radiosity are calculated for each surface and a set of energy balance equations for internal and external surfaces are written. In this work, it is assumed that the collector mirror temperature is approximately the ambient temperature. When the collector surface is not included in the analysis, maximum radiation heat transfer loss occurs, and this means that the glass envelope is assumed to be totally covered by the sky. So, the heat flux (\dot{q}_{esi}) for the area considered is expressed by Stefan-Boltzmann's equation:

$$\dot{q}_{esi} = \sigma \varepsilon_{esi} (T_{esi}^4 - T_{sky}^4) \quad (16)$$

where σ is Stefan-Boltzmann constant ($5.67 \times 10^{-8} \text{ W /m}^2\text{K}^4$), ε is the object emissivity, T_{esi} is body temperature, T_{sky} ambient temperature.

Several relationships have been proposed to connect T_{sky} for clear skies, to other meteorological variables. In the absence of meteorological data such as relative humidity, dew point temperature, etc., a simple relation given by Swinbank [32] can be used:

$$T_{sky} = 0.0553 T_{\infty}^{1.5} \quad (17)$$

The energy absorbed in the solar receiver is affected by optical properties and imperfections of the solar collector ensemble. For a concentrating collector, the effective optical efficiency is defined as long as the direct beam radiation is normal to the collector aperture area. When the beam radiation is not normal, the angle of incidence modifier (IAM) is included to account for optical and geometric losses due to angles of incidence greater than 0° . The IAM depends on geometrical and optical characteristics of the solar collector. It is defined as the quotient between the transmittance-absorptance product at the angle of the incidence of radiation and that at normal incident radiation.

3. NUMERICAL MODEL

The set of partial differential equations (PDE) was discretized for steady state conditions by using the finite difference method and taking into account the dependence of thermal properties on temperature. Turning to the heat transfer fluid, discretization by backward differencing creates a set of algebraic equations. For the absorber and the envelope, the discretization is carried out using the central difference and thus, another set of algebraic equations is obtained. Finally, the boundary conditions for each element are set down.

The proposed model includes the thermal interaction between absorber-envelope, and envelope-envelope. These thermal radiation losses were not included in other existing models. To account for the thermal interaction between adjacent surfaces, a comprehensive radiative analysis was implemented for heat losses in the absorber and the glass envelope. A review of the equations for convective heat transfer loss was performed as well, and new equations were incorporated to the present model. The effects of heat conduction in the collector tube wall and the mixed convection in the inner tube, which have been neglected in previous studies, are also taken into consideration in the present model. The resulting set of nonlinear algebraic equations is solved simultaneously using numerical techniques. These equations are solved using an implicit Euler scheme. Linear system equations are written

using the matrix-vector notation, $Ax = b$, where A is the matrix of coefficients for the system, x the column vector of the unknown variables x_1, \dots, x_n , and b a given column vector.

Collector thermal efficiency (η) is defined as the ratio of energy collected by the working fluid to the direct normal solar radiation incident upon the collector aperture. It is typically determined by testing a collector over a range of high temperatures and is expressed as:

$$\eta = \frac{\dot{m}(T_{o,f} - T_{i,f})}{GA_a} \quad (18)$$

Where where \dot{m}_f is the fluid mass flow rate, $T_{o,f}$ fluid outlet temperature, $T_{i,f}$ fluid inlet temperature, G is global solar radiation on collector surface (W/m^2) and A_a is the absorber area. The thermal loss from the collector receiver is related to the operating temperature. The thermal loss through PTSC can be changed in different ways depending on the receiver's configuration and operational conditions. The thermal loss can be expressed as:

$$\text{Thermal loss} = \sum_i (\dot{Q}'_{a-e,conv})_i + \sum_i (\dot{Q}'_{e-s,rad})_i + \sum_j (\dot{Q}'_{cond,bracket})_j \quad (19)$$

where $\dot{Q}'_{a-e,conv}$ is the heat transfer by convection from the glass envelope to the surrounding air per unit length, and, $\dot{Q}'_{e-s,rad}$ is the heat transfer by radiation from the glass envelope to sky per unit length and $\dot{Q}'_{cond,bracket}$ is the heat conduction through support brackets per unit length.

A simulation model compatible with the transient simulation program (TRNSYS) was developed to determine the thermal performance of a typical parabolic trough configuration under Kuwait climatic conditions. A TRNSYS Studio project is designed by setting up the connecting components graphically in the simulation study as explained by Klein et al. [33]. Parameters treated were: area of collector's absorber, overall heat loss coefficient from the absorber, reflectivity of the reflecting surface and absorptivity and emissivity of the absorber. The parametric study was conducted for different mass flow rates and concentration ratios utilizing hourly solar radiation data for Kuwait. The processed solar insolation data consist of the beam radiation and diffuse radiation as well as the total radiation on a tilted surface measured in W/m^2 .

4. RESULTS AND DISCUSSIONS

In order to validate the present heat transfer model, it was first compared with experimental data obtained by Dudley et al. [34]. In addition, to corroborate the improvement in the equations and radiation analysis proposed here, García Valladares et al. [35] compared the numerical model results against those from other solar receiver heat transfer models. The experimental results were obtained from a solar collector assembly module (LS-2) placed on an AZTRAK rotating platform at the SNL. Two different selective coatings were used in this test: black chrome and cermet. Cermet has better radiative properties (low emissivity) at high temperatures than black chrome and does not oxidize if the vacuum is lost.

The Sandia test was performed for both: Full sun and no sun conditions and different scenarios for the annulus of the heat collection element (HCE). Among them: vacuum intact (*In vacuo*), with annulus pressure at 10^{-4} Torr, lost vacuum (annulus filled with ambient air),

and glass cover completely removed (bare tube). Fig. 2 presents the results obtained for the collector efficiency. As seen in the figure, the current calculated collector efficiency follows the trend of the experimental values and all of the results are within the error bars. As expected, the higher efficiencies are obtained when the annulus is *In vacuo*, but in both cases, air and vacuum, the collector efficiency drops gradually at high temperature. This behavior is more noticeable for black chrome coating.

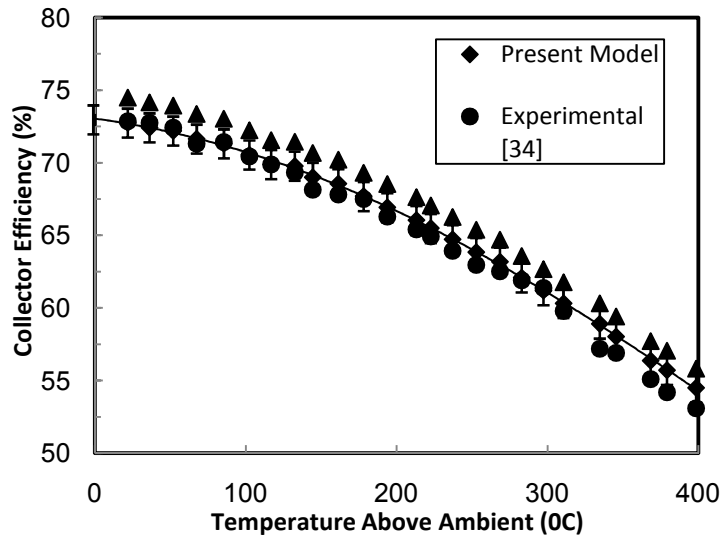


Fig. 2. Comparison of collector efficiency as calculated with the proposed model to experimental data [34] and NREL model [35]

In case of Cermet coating, the model developed by García-Valladares and Velásquez [35] shows some discrepancies at low temperatures in the collector efficiency. These discrepancies may be attributed to their assumptions: negligible conduction at each end of each trough and that only radiation heat loss takes place between the receiver and the glass envelope for *In vacuo* annular space. These assumptions were made neither in the present nor in the NREL model. So, the present model and NREL model introduced by Dudley et al. [34] give almost similar collector efficiency values.

The angle of incidence modifier, $K_{gr}(\theta_i)$, enables the performance of the collector to be predicted for solar angles of incidence other than 0° (normal). Simulations using the present numerical model are carried out setting up a value of θ_i and then calculating K_{gr} .

The angle of incidence modifier represents the ratio between a specified thermal efficiency value and the peak efficiency of the collector at zero incidence. Results of simulation are presented in Fig. 3. Regression analyses provided the following equations for K_{gr} as a function of θ_i :

$$K_{grU} = -2.235 \times 10^{-6}(\theta_i)^3 + 1.2146 \times 10^{-4}(\theta_i)^2 - 3.884 \times 10^{-3}(\theta_i) + 1.125 \quad (20)$$

$$K_{grG} = 9.272 \times 10^{-7}(\theta_i)^3 - 1.561 \times 10^{-4}(\theta_i)^2 + 1.773 \times 10^{-3}(\theta_i) + 1.078 \quad (21)$$

Coefficients upon solving equations (20) and (21) were 0.958 and 0.961. Up to an angle of incidence of approximately 25° the glass-shielded receiver performed slightly better but, for greater angles, performance declined more rapidly and was inferior to that of the unshielded receiver.

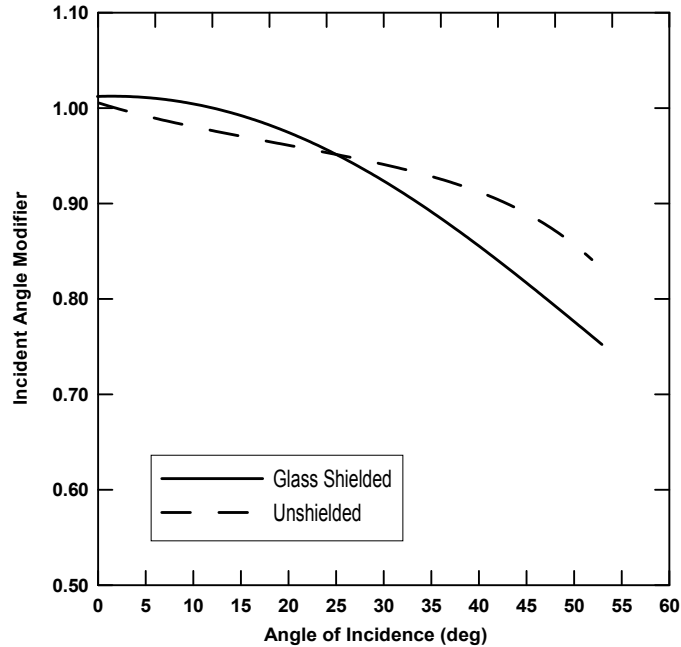


Fig. 3. The angle of incidence modifier for unshielded and glass-shielded receivers

In Fig. 3, the calculated value of K_{gr} was 0.74 for the glass-shielded receiver at the maximum tested incidence angle of 54° , an 8.9% lower than that for the unshielded receiver. At the same maximum angle of incidence, the simplified cosine model under-predicted K_{gr} by about 25% for the unshielded receiver and by 17.7% for the glass shielded unit. Two factors are primarily responsible for the decline in performance of a PTSC with increasing θ_i : the geometric reduction in irradiance falling on the aperture as θ_i increases or 'cosine effect' and the change in optical efficiency (due to differences in light interaction) with the reflective surface of the collector, the glass shield (if present) and the absorber. Nothing can be done to account for the first effect other than tilting the PTSC constantly so as to keep it perpendicularly oriented to the sun.

The thermal losses of the collector receiver depend on operating temperature. The thermal losses through PTSC change in different ways depending on the receiver's configuration and operational conditions. As shown in Fig. 4, the convection loss from the absorber tube to supporting structures is the largest. It follows in decreasing order the radiation loss from the glass envelope to ambient air, while the smaller loss is the convection loss from the glass envelope to ambient air. Thermal losses are always present if there is a temperature difference between receiver and ambient whether solar radiation is available or not.

Increased solar radiation results in increased solar energy absorbed by the collector. It should be noted that thermal losses also increase due to the increased collector temperature. However, this increase is smaller than the enhanced absorbed solar energy. As shown from Fig. 5, PSTC efficiency increases with increasing solar radiation.

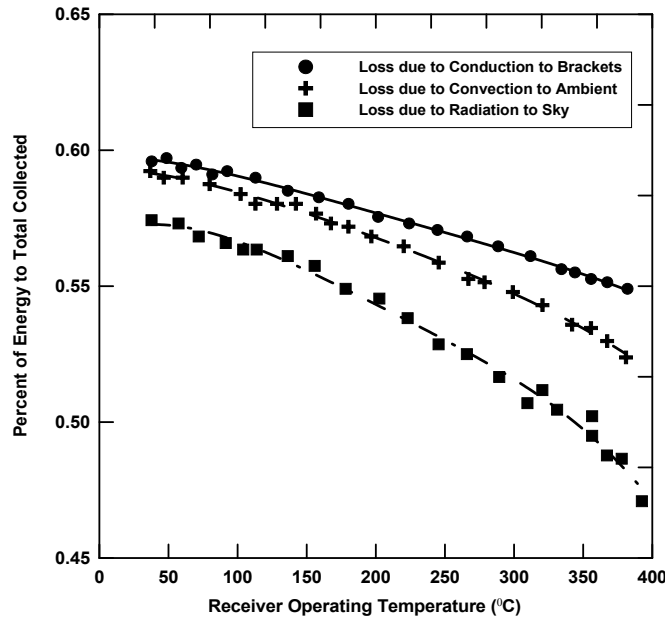


Fig. 4. Heat loss from an absorber tube

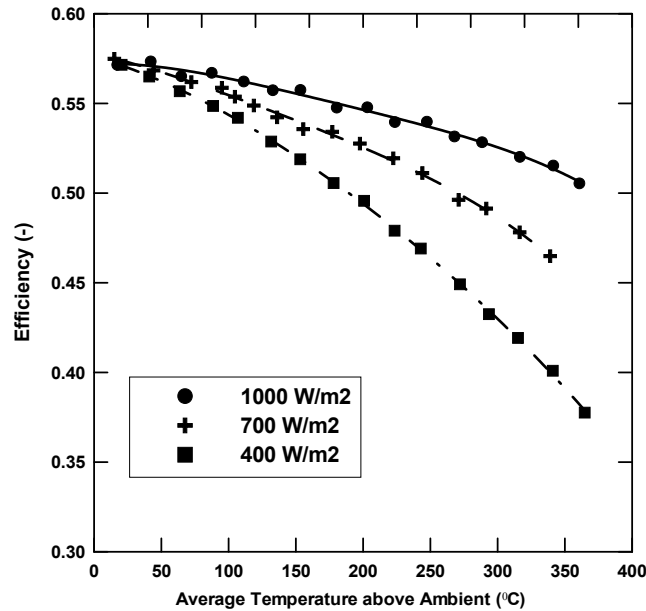


Fig. 5. Variation of parabolic trough collector efficiency with solar radiation

The angle of incidence modifier (IAM) is a very significant factor impacting on the solar efficiency, and can be approximately estimated as the cosine of the angle of incidence. IAM depends on time of day, date, the location and orientation of the aperture, and whether the collector is stationary or tracks the sun movement about one or two axes. Collector efficiency reaches a maximum value only at zero angle of incidence. The efficiency of a PTSC decreases when the angle of incidence of solar beam increases, as shown in Fig. 6. The

effect of the angle of incidence is to reduce radiation arriving at the absorber tube. Therefore, at noon time PTSC has the smallest angle of incidence and the highest efficiency.

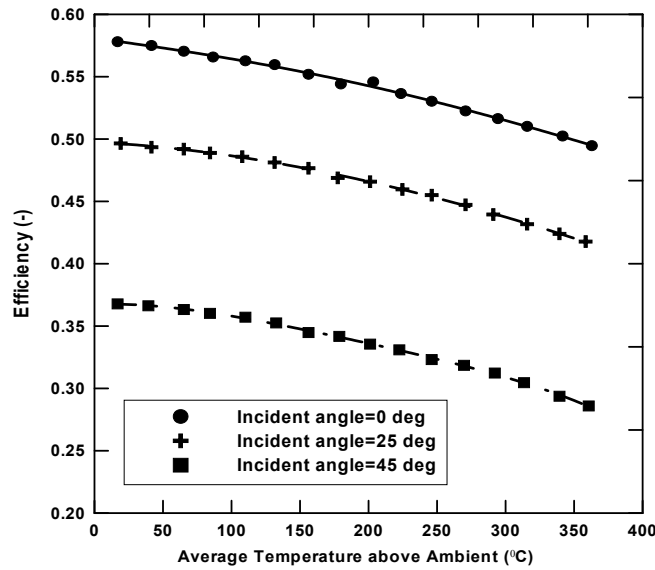


Fig. 6. Variation of collector efficiency with angle of incidence

When the annulus between the receiver surface and the glass envelope is in vacuum state, conduction and convection across the annulus are effectively eliminated. Once air is introduced into the vacuum space, measured losses increase significantly since conduction and convection begin to transfer heat to the glass envelope as shown in Fig. 7. Radiation loss from the heated receiver's metal surface to the glass envelope does not change significantly when air is allowed into the annulus.

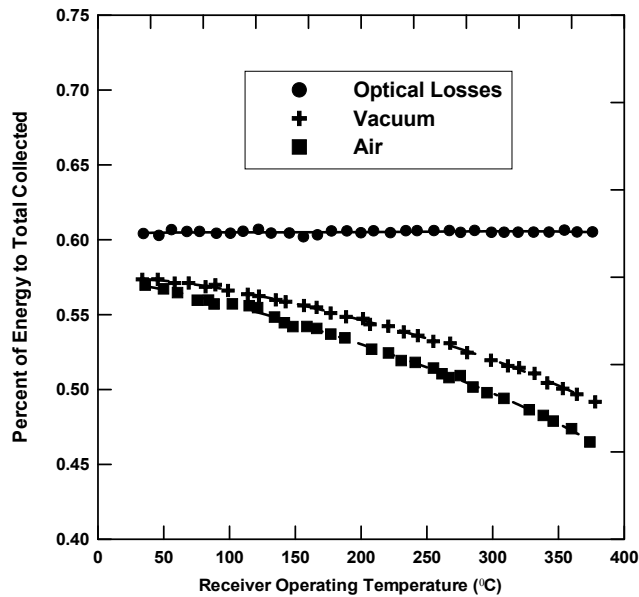


Fig. 7. Collector efficiency with air in annulus

5. CASE STUDY

A case study is carried out to investigate the performance of solar heating and cooling systems in Kuwait. The solar system is designed to satisfy a significant part of the nominal space heating load, water heating load and cooling load of a typical Kuwaiti house. A schematic diagram of the system studied is represented in Fig. 8. The system consists of parabolic trough collectors integrated into the roof of the building, a storage tank, an absorption chiller, heat exchanger and auxiliary units. The main purpose of this stage is to investigate the feasibility of integrating parabolic trough collectors in an existing building in order to convert it to nearly zero net energy building.

Buildings are responsible for a significant part of the total primary energy consumption. Thus, researchers and designers thrive to develop energy efficient buildings from renewable energy sources. Many new buildings incorporate solar energy technology to attain environmental goals as opposed to conventional energy in order to reduce greenhouse and other gases emission, mainly CO₂ as presented by Zhai et al. [36], Yin et al. [37], Thomas et al. [38], Bourrelle et al. [39], Bucking et al. [40] and, Zeiter et al. [41].

A solar heating and cooling system operates in four different modes. When solar energy is available for collection and there is load demand, heat is supplied directly from the collector to the heating or cooling unit. When solar energy is available for collection and there is no heat or cooling demand, heat is stored in the storage unit. On the other hand, if solar energy is not available for collection and there is load demand, the storage unit then supplies heat to the heating or cooling unit. However, if the storage temperature is not sufficient, the heating or cooling load is supplied by the auxiliary source.

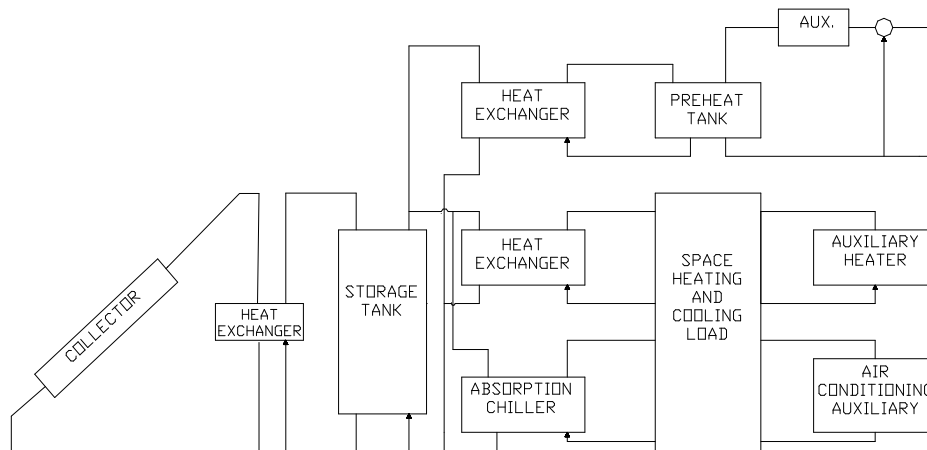


Fig. 8. Schematic diagram of a solar heating and cooling system

The solar cooling system consists of single-effect lithium bromide water absorption chiller. The chiller model is based on a commercially available LiBr-H₂O absorption chiller system, Arkla model WF-36. The Arkla chiller has a nominal cooling capacity of three tons (37980kJ/h). Units of different capacity are approximated by scaling the Arkla performance. Hot water is supplied to the air conditioner at temperatures ranging between 87°C and 93°C, leaving this unit 10°C cooler than the supply and ending into the storage, or to the auxiliary heater if storage temperature is below 77°C. Whenever hot water from the storage

temperature is below 87°C, auxiliary heat is supplied to raise its temperature to 87°C. When storage temperature is below 77°C, it is not used, and the auxiliary heater carries the full cooling load.

The performance of air conditioning systems is expressed by their coefficient of performance (COP). COP determines how many units of cooling/heating is attained for every unit of input energy. In addition, a constant COP model of a vapor compression air conditioner is included as a secondary cooling auxiliary unit, so that the energy required to meet space cooling is always provided even if the absorption machine cannot meet the full load.

5.1 Building load

The model dwelling under study is a typical Kuwaiti house in a remote area. The computer program is provided with an estimate of typical loads encountered in the house. An hourly load schedule is written to an input file. The program is provided with an estimate of the number of hours that the load is utilized during a typical day for each load. The roof area is large enough so that the parabolic trough collectors can be spaced widely to minimize shading losses. The domestic water demand is based on a figure of 60 kg/day/person. The system has been designed to supply cooling up to a load peak of about 21 kW (6 tons of refrigeration), which occurs in August.

Different collector parameters and operating conditions were essayed to maximize the annual energy generated by the parabolic trough collector. For building simulation, type 56 included in version 16 of TRNSYS developed by Klein et al. [33] is employed. This component models the thermal behavior of a building with multiple thermal zones. The building can be completely described using this component from a set of external files. The files can be generated based on user supplied information by running the preprocessor program called TRN Build.

From simulation with TRN build (Type 56) of TRNSYS to determine the building's demand for air conditioning, results indicate that this demand spans from April to October, with critical periods of maximum load in the months of June, July and August. Study results showed that the air conditioning system consumed about 83% of the total building energy requirement. The remaining energy consumption is distributed between space heating 11%, and domestic water heating, 6%. For hot thermal storage, a stratified liquid storage tank, with two flow inlet and two flow outlet, Type 60, is adapted. Several data files of single-effect absorption chillers employing LiBr-H₂O solution as working fluid, (type 107) according to Yazaki chiller WFC SH10 are used. Other model types essayed were: Type 15, TMY2 and Type 3b for pump simulation.

5.2 Solar Fraction

The thermal performance of a solar system is usually measured by the solar fraction (F). Solar fraction is defined as the fraction of the load met by solar energy. Fig. 9 shows the variation of solar fraction of space heating (F_s), domestic water heating (F_D), and cooling load (F_{Ac}) with collecting area. As seen from the figure, the solar space heating load and domestic water heating load are completely satisfied for areas of about 29 m². Conversely, the space cooling load requires much greater areas. The minimum required collector area is about 82 m² which can supply the cooling load of a typical residential house for sunshine hours under all hot weather conditions in Kuwait, with a maximum cooling load of approximately 21 KW (6 ton refrigeration).

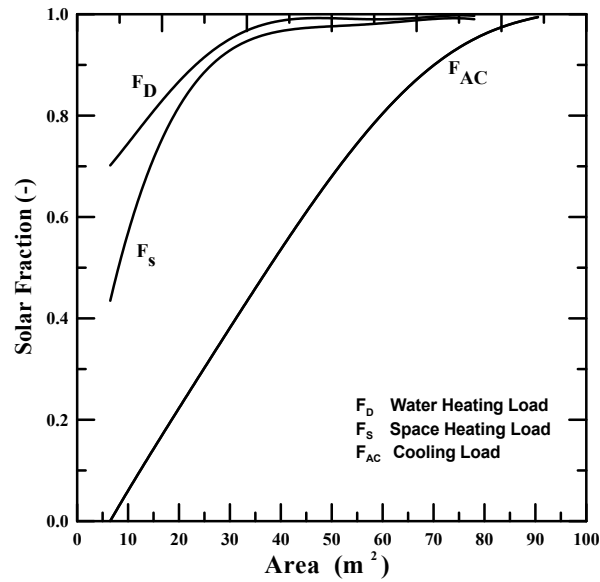


Fig. 9. Solar fraction variation with collecting area

The coefficient of performance (COP) of the absorption chiller is approximately 0.66 which is within the accepted practical values of the conventional lithium bromide system.

A computer routine was developed to determine the yearly reduced CO₂ emission as a result of integrating parabolic trough collectors on the house roof. The annual variation of CO₂ decreased emission vs. collector area is presented in Fig. 10. In this figure at collecting area values satisfying house cooling load, the calculated CO₂ emissions reduction was 12.3tonne/year.

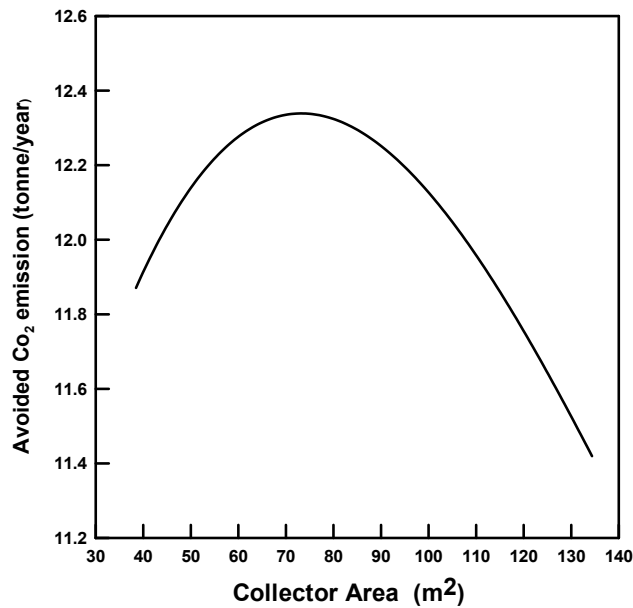


Fig. 10. CO₂ emissions reduction variation with collecting area at zero azimuth Angle

6. CONCLUSIONS

This paper investigates the performance of parabolic trough collectors as well as solar heating and cooling systems in Kuwait climate. A theoretical model that takes into consideration some factors not included in previous models is proposed. Based on present results, the following conclusions can be drawn:

- The performance of parabolic trough collectors can be significantly enhanced by optimizing its parameters as well as operating conditions. Reducing the heat transfer losses can significantly improve collector efficiency.
- Convection loss from the absorber tube to the supporting structures is the largest among the other losses (conduction and radiation).
- The angle of incidence modifier is an important factor impacting on the solar efficiency. At temperature 150°C, parabolic trough collector efficiency decreases from about 0.55 at angle of incidence 0° to about 0.35 at angle of incidence 45°.
- At noon time, PTSC has the smallest angle of incidence and the highest efficiency.
- When the annulus between the receiver surface and the glass envelope is *In vacuo*, conduction and convection across the annulus are effectively eliminated.
- Space and domestic water heating loads can be completely provided by parabolic trough collectors.
- The minimum required parabolic trough collecting area is about 82 m² to supply cooling loads of a typical residential house under all climatic conditions in Kuwait.
- Total reduction in CO₂ emission may reach to some 12.3tonne/year per building.
- The results of the present study should encourage widespread utilization of solar energy systems which will help in keeping our environment healthy and clean.

ACKNOWLEDGEMENTS

The authors would like to express their sincere gratitude to the Public Authority for Applied Education and Training (PAAET), Kuwait for supporting and funding this work, Research Project No. (TS-11-09), Research Project Title "Assessment of Parabolic Trough Collector Performance in Kuwait Climate".

COMPETING INTERESTS

Authors declare that there are no competing interests.

REFERENCES

1. Kalogirou S, Lloyd S, Ward J. Modeling, Optimization and Performance Evaluation of a Parabolic Trough Solar Collector Steam Generation. *Solar Energy*. 1997;60(1):49-59.
2. Price H, Lupfert E, Kearney D, Zarza E, Cohen G, Gee R, Mahoney R. Advances in Parabolic Trough Solar Power Technology. *Journal of Solar Energy Engineering*. 2002;124:109-125.

3. Riffelmann K, Neumann A, Ulmer S. Performance Enhancement of Parabolic Trough Collectors by Solar Flux Measurement in the Focal Region. *Solar Energy*. 2006;80:1303–1313.
4. Eck M, Zarza E. Saturated Steam Process with Direct Steam Generating Parabolic Troughs. *Solar Energy*. 2006;80:1424–1433.
5. Mazloumi M, Naghashzadegan M, Javaherdeh K. Simulation Study of Solar lithium bromide–water absorption cooling system with parabolic trough collector. *Energy Conversion and Management*. 2008;49:2820-2832.
6. Adinberg R, Zvegilsky D, Epstein M. Heat transfer efficient thermal energy storage for steam generation. *Energy Conversion and Management*. 2010;51:9-15.
7. Garcí'a A, Zarza E, Valenzuela L, Rez M. Parabolic-Trough Solar Collectors and Their Applications. *Renewable and Sustainable Energy Reviews*. 2010;14:1695–1721.
8. Sansoni P, Fontani D, Francini, F, Giannuzzi A, Sani E, Mercatelli L, Jafrancesco D. Optical Collection Efficiency and Orientation of a Solar Trough Medium-Power Plant Installed in Italy. *Renewable Energy*. 2011;36:2341-2347.
9. Daniel P, Joshi Y, Das A. Numerical Investigation of Parabolic Trough Receiver Performance with Outer Vacuum Shell. *Solar Energy*. 2011;85:1910–1914.
10. Forristall R. Heat Transfer Analysis and Modeling of a Parabolic Trough Solar Receiver Implemented in Engineering Equation Solver. National Renewable Energy Laboratory (NREL), Colorado; 2003.
11. Jones S, Pitz-Paal R, Schwarzboezl P, Hohe L, Blair N, Cable R. TRNSYS Modeling of the SEGS VI Parabolic Trough Solar Electric Generating System. In *Proceedings of Solar Forum: Solar Energy: The Power to Choose*, Washington, DC, USA. 2011;405.
12. Li Xu, Wang Z, Xin Li, Yuan G, Sun F, Lei D. Dynamic test model for the transient thermal performance of parabolic trough solar collectors. *Solar Energy*. 2013;95:65-78.
13. Blair N, Mehos M, Christensen C. Sensitivity of Concentrating Solar Power trough performance, cost, and financing with the Solar Advisor Model. Tech. Rep. NREL/CD-550-42709, NREL; 2008.
14. National Renewable Energy Laboratory (NREL), Solar Advisor Model CSP Reference Manual for Version 3.0; 2009.
15. Montes M, Abánades A, Martínez-Val J, Valdés M. Solar multiple optimization for a solar-only thermal power plant, using oil as heat transfer fluid in the parabolic trough collectors. *Solar Energy*. 2009;83(12):2165 – 2176.
16. Rolim MM, Fraidenaich N, Tiba C. Analytic modeling of a solar power plant with parabolic linear collectors. *Solar Energy*. 2009;126–133.
17. Harrigan R, Handbook for the conceptual design of parabolic trough solar energy systems process heat applications. Tech. rep., NASA STI/Recon Technical Report; 1981.
18. Edenburn MW. Performance analysis of a cylindrical parabolic focusing collector and comparison with experimental results. *Solar Energy*. 1976;18(5):437–444.
19. Pope R, Schimmel. An analysis of linear focused collectors for solar power. In *Eighth Intersociety Energy Conversion Engineering Conference*, Philadelphia, PA. 1973:353–359.
20. Ratzel A, Hickox C, Gartling D. Techniques for reducing thermal conduction and natural convection heat losses in annular receiver geometries. *J Heat Transfer Trans ASME*. 1979;101(1):108–113.

21. Dudley V, Kolb G, Sloan M, Kearney D. SEGS LS2 Solar Collector-Test Results. Report of Sandia National Laboratories, SAN94-1884; 1996.
22. Stuetzle T. Automatic control of the 30MWe SEGS VI parabolic trough plant. Master's thesis, University of Wisconsin-Madison, College of Engineering; 2002.
23. García-Valladares O, Velázquez N. Numerical simulation of parabolic trough solar collector: Improvement using counter flow concentric circular heat exchangers. *International Journal of Heat and Mass Transfer*. 2009;52(3-4):597–609.
24. Heidemann W, Spindler K, Hahne E. Steady-state and transient temperature field in the absorber tube of a direct steam generating solar collector. *International Journal of Heat and Mass Transfer*. 1992;35(3):649–657.
25. Odeh S, Morrison G, Behnia M. Thermal analysis of parabolic trough solar collectors for electric power generation. In *Proceedings of ANZSES 34th annual conference*, Darwin, Australia. 1996;460–467.
26. Cheng Z, He Y, Xiao J, Tao Y, Xu R. Three-dimensional numerical study of heat transfer characteristics in the receiver tube of parabolic trough solar collector. *International Communications in Heat and Mass Transfer*. 2010;37(7):782–787.
27. He Y, Xiao J, Cheng Z, Ao Y. A MCRT and FVM coupled simulation method for energy conversion process in parabolic trough solar collector. *Renewable Energy*. 2011;36:976–985.
28. Gong G, Huang X, Wang J, Hao M. An optimized model and test of the China's first high temperature parabolic trough solar receiver. *Solar Energy*. DOI: 10.1016/j.solener.2010.08.003; 2010.
29. Rohsenow WM, Hartnett J P, Cho Y I. *Handbook of Heat Transfer*, 3 ed. McGraw-Hill Professional May; 1998.
30. Kakaç S, Shah RK, Aung W. *Handbook of Single-Phase Convective Heat Transfer*. John Wiley & Sons, New York; 1987.
31. Siegel R, Howell, J R. *Thermal Radiation Heat Transfer*. McGraw-Hill, New York; 1971.
32. Swinbank W. Long-wave radiation from clear skies. *Quarterly Journal of the Royal Meteorological Society*. 1963;89(381):339–348.
33. Klein SA et al. : *TRNSYS : A Transient Simulation Program*", Version 16, University of Wisconsin-Madison; 2006.
34. Dudley V, Kolb G, Sloan M, Kearney D. 1994. SEGS LS2 Solar Collector-Test Results. Report of Sandia National Laboratories. SAN94-1884;1994.
35. García-Valladares O, Velázquez N. Numerical simulation of parabolic trough solar collector: improvement using counter flow concentric circular heat exchangers. *Int J Heat Mass Trans*. 2009;52:597–609.
36. Zhai X Q, Wang R, Dai YJ, Wu JY. Experience on integration of solar thermal technologies with green buildings. *Renewable Energy*. 2008;33:1904–1910.
37. Yin HM, Yang DJ, Kelly G, Garant J. Design and performance of a novel building integrated PV / thermal system for energy efficiency of buildings. *Solar Energy*. 2013;87:184-195.
38. Thomas D, Duffy J. Energy performance of net-zero and near net-zero energy homes in New England. *Energy and Building*. 2013;67:551-558.
39. Bourrelle J, Andresen I, Gustavsen A. Energy payback: An attributional and environmentally focused approach to energy balance in net zero energy buildings. *Energy and Building*. 2013;65:84-92.

40. Bucking S, Zmeureanu R, Athienitis A. An information driven hybrid evolutionary algorithm for optimal design of a Net Zero Energy House. *Solar Energy*. 2013;96:128-139.
41. Zeiter W, Boxem G. Net-zero energy building schools. *Renewable Energy*. 2013;49:282-286.

© 2014 Akan et al.; This is an Open Access article distributed under the terms of the Creative Commons Attribution License (<http://creativecommons.org/licenses/by/3.0>), which permits unrestricted use, distribution, and reproduction in any medium, provided the original work is properly cited.

Peer-review history:

The peer review history for this paper can be accessed here:
<http://www.sciencedomain.org/review-history.php?iid=468&id=5&aid=4083>